2D numerical modelling of dam break- applying for Namchien dam in Vietnam

Le Thi Thu Hien; Quang Hung Nguyen

Abstract*: *The paper is dedicated to study a numerical model simulating dam-break based on two dimensional nonlinear shallow water equations (2D-NSWE). Finite Volume Method-Godunov type is applied to discretize this equation. Roe scheme is utilized to approximate Riemann problem, meanwhile method of flux difference splitting is implemented to construct numerical solvers of SWE. Besides, the semi implicit scheme is also invoked to solve friction term in case of high roughness coefficient. The proposed model is verified through a comparison between computed results and empirical data of two reference tests. A dam break flow over floodable area with different roughness coefficients is also researched. A total collapsed dam scenario of an arch dam-Nam Chien in Vietnam is simulated by the proposed model. Several hydraulic characteristics such as flood extent, arrival time and time histories of water depth at different gauges are estimated with different grid sizes.

Keywords*: *Shallow water equations; Finite Volume Method; dam break; Nam Chien

I. INTRODUCTION

Flood risk management has been established to provide a well-designed plan to warn, prevent, monitor and control flood risk, which in turn needs a reliable flood risk assessment, [1, 2]. Nowadays, numerical methods are a widespread tool for studying physical problems that can be mathematically modelled by a set of partial different equations. Among several applications, in hydraulic engineering numerical modelling based on Shallow Water Equations (SWE) is frequently adopted for river basin management, hazard risk assessment and then provide emergency plans in the case of catastrophic events, like river inundation, dike failures or dam breaks, [3, 4]. Several techniques of computational fluid dynamics have been developed in some recent decades to solve SWE, such as Finite Difference Method (FDM), Finite Element Method (FEM) or Finite Volume Method (FVM). Finite Volume Method (FVM) solving Partial Differential Equations (PDE) in the form of integral equations, recently, is considered as the most widely used numerical strategy in solving 2D SWE, [5, 6]. The computational domain is discretized into a certain number of mesh cells and the integral form of SWE is implemented for each cell. The flux through the boundaries of the cells is approximated to update variables at every time step. This procedure makes sure the conservation of mass and momentum, is extremely flexible and conceptually simple. Numerous researchers have applied FVM to real case studies simulated water propagation over arbitrary topographies, [7-12]. Besides, the numerical simulation of natural case study is characterized by several problems, such as: complex geometry, high roughness coefficient or wet/dry front. Dam-break problem over real geometrical irregularities and rough bottom is always considered as a big challenge in simulating flood wave on downstream. The complicated geometry may generate unphysical solution in simulating flood flow propagation. Thus, a stable algorithm, can work with two dimensional domain and provide shock-capturing capability is necessary, [7]. Therefore, in this article, FVM with Godunov type is utilized and Flux Different Splitting Method (FDS) is invoked in order to make the exactly balance between fluxes terms and source terms. Besides, friction term is solved by semi implicit scheme. Two experiment tests introduced are reproduced to verify the proposed numerical scheme, [13, 14]. On the other hand, the influence of sensitivity of roughness coefficient on hydraulic characteristic is also validated by a case study. The effectiveness and robustness indicated by comparing numerical results with observed ones of two test cases, indicating good application capability is an important goal of this research. A dam break scenario of a unique arch dam in Vietnam – Nam Chien is selected to check the capability of the present numerical model. Several hydraulic characteristics are estimated such as: water depth profile, flooding maps, arrival time, peak of water level. From that an early warning can be proposed for hydropower plant located at downstream valley of Nam Chien reservoir is indicated.

II. NUMERICAL MODEL

A. Mathematical scheme

The vetor form of 2D SWE can be expressed by:

$$\frac{\partial \mathbf{V}}{\partial t}+\frac{\partial \mathbf{K}(\mathbf{V})}{\partial x}+\frac{\partial \mathbf{H}(\mathbf{V})}{\partial y}=\mathbf{S}_1(\mathbf{V})+\mathbf{S}_2(\mathbf{V}) \quad (1)$$

In (1), **V** is the vector of conserved variables; **K** and **H** are flux vectors; $\mathbf{S}_1$ and $\mathbf{S}_2$ are two terms of bed slope and friction.

$$\mathbf{V}=[h;\ hu;\ hv]^T;\ \mathbf{K}(\mathbf{V})=\left[hu;\ hu^2+0.5gh^2;\ huv\right]^T;$$
$$\mathbf{H}(\mathbf{V})=\left[hv;\ huv;\ hv^2+0.5gh^2\right]^T \quad (2)$$

Revised Manuscript Received on July 05, 2019.
Le Thi Thu Hien, Thuyloi University, 100000 Ha noi, Vietnam.
Quang Hung Nguyen, Thuyloi University, 100000 Ha noi, Vietnam.

Published By:
Blue Eyes Intelligence Engineering
& Sciences Publication

$$\mathbf{S}_1(\mathbf{V}) = [0; -gh\partial z_b/\partial x; -gh\partial z_b/\partial y]^T = \mathbf{S}_{1x} + \mathbf{S}_{1y}$$
$$= [0; -gh\partial z_b/\partial x; 0]^T + [0; 0; -gh\partial z_b/\partial y]^T \quad (3)$$
$$\mathbf{S}_2(\mathbf{V}) = [0; -\tau_x/\rho; -\tau_y/\rho]^T$$

in which τ_x and τ_y are bottom shear stress given by:

$$\tau_x = \rho C_f u\sqrt{u^2+v^2};\ \tau_y = \rho C_f v\sqrt{u^2+v^2};$$
$$C_f = \frac{g.n^2}{h^{1/3}} \quad (4)$$

where: h is water depth, u and v are the velocity components in x and y directions; z_b is bed elevation; n is Manning roughness parameter; g is the acceleration of gravity.

Using the Jacobian matrix, 2D SWE can be rewritten in the *quasi-linear form*:

$$\frac{\partial \mathbf{V}}{\partial t} + \mathbf{M}(\mathbf{V})\frac{\partial \mathbf{V}}{\partial x} + \mathbf{N}(\mathbf{V})\frac{\partial \mathbf{V}}{\partial y} = \mathbf{S}(\mathbf{V}) \quad (5)$$

Where $\mathbf{M}(\mathbf{V})$ and $\mathbf{N}(\mathbf{V})$ are Jacobian matrices corresponding to the fluxes $\mathbf{K}(\mathbf{V})$ and $\mathbf{H}(\mathbf{V})$, respectively. The expressions of two matrices are:

$$\mathbf{M}(\mathbf{V}) = \frac{\partial \mathbf{K}}{\partial \mathbf{V}} = \begin{bmatrix} 0 & 1 & 0 \\ a^2 - u^2 & 2u & 0 \\ -uv & v & u \end{bmatrix};$$
$$\mathbf{N}(\mathbf{V}) = \begin{bmatrix} 0 & 0 & 1 \\ -uv & v & u \\ a^2 - v^2 & 0 & 2v \end{bmatrix} \quad (6)$$

where $a = \sqrt{gh}$ is the celerity.

In general, the Eq. (6) is not a linear system if the components of $\mathbf{M}$ and $\mathbf{N}$ depend on variable $\mathbf{V}$. Otherwise, if all components of these matrices are constant, we obtain a linear system.

B. Numerical scheme

The conserved variables $\mathbf{V}$ are simulated to a new time step by the Eq. 7, based on Godunov type,

$$\mathbf{V}_{i,j}^{k+1} = \mathbf{V}_{i,j}^{k} - \frac{\Delta t}{\Delta x}\left[\mathbf{K}_{i+1/2,j} - \mathbf{K}_{i-1/2,j}\right]$$
$$-\frac{\Delta t}{\Delta y}\left[\mathbf{H}_{i,j+1/2} - \mathbf{H}_{i,j-1/2}\right] + \Delta t\mathbf{S}_{1i,j} + \Delta t\mathbf{S}_{2i,j} \quad (7)$$

where superscripts k denote time levels; subscripts i and j are space indices along x and y directions; Δt, Δx, Δy are time step and space sizes of the computational cell.

FDS method is constructed to guarantee an exact balance between the bed slope terms and the flux gradients when solving SWE, [15]. The discretisation is performed so that retains an exact balance between flux gradients and source terms; Roe scheme is selected for approximation flux terms, $\mathbf{K}_{i\pm1/2,j}$; $\mathbf{H}_{i,j\pm1/2}$.

Two components of bed slop terms are discretized by Eq. 8 and Eq. 9.

$$\tilde{\mathbf{S}}_{1x} = \tilde{\mathbf{S}}_{1x}^{+} + \tilde{\mathbf{S}}_{1x}^{-} = -\frac{g\tilde{h}}{4\tilde{c}}\frac{\Delta z_{bx}}{\Delta x}\left\{\begin{bmatrix} sign(\lambda) - sign(\beta) \\ 2\tilde{c} + |\lambda| - |\beta| \\ \tilde{v}[sign(\lambda) - sign(\beta)] \end{bmatrix} + \begin{bmatrix} -sign(\lambda) + sign(\beta) \\ 2\tilde{c} - |\lambda| + |\beta| \\ \tilde{v}[-sign(\lambda) + sign(\beta)] \end{bmatrix}\right\} \quad (8)$$

where $\lambda = \tilde{u} + \tilde{c}; \beta = \tilde{u} - \tilde{c}$

$$\tilde{\mathbf{S}}_{1y} = \tilde{\mathbf{S}}_{1y}^{+} + \tilde{\mathbf{S}}_{1y}^{-} = -\frac{g\tilde{h}}{4\tilde{c}}\frac{\Delta z_{by}}{\Delta y}\left\{\begin{bmatrix} sign(\alpha) - sign(\varepsilon) \\ \tilde{u}[sign(\alpha) - sign(\varepsilon)] \\ 2\tilde{c} + |\alpha| - |\varepsilon| \end{bmatrix} + \begin{bmatrix} -sign(\alpha) + sign(\varepsilon) \\ \tilde{u}[-sign(\alpha) + sign(\varepsilon)] \\ 2\tilde{c} - |\alpha| + |\varepsilon| \end{bmatrix}\right\} \quad (9)$$

where $\alpha = \tilde{v} + \tilde{c}; \varepsilon = \tilde{v} - \tilde{c}$

Average value of water depth, velocity components and celerity are taken by (10) [16].

$$\tilde{u} = \frac{\sqrt{h_R}u_R + \sqrt{h_L}u_L}{\sqrt{h_R} + \sqrt{h_L}}$$
$$\tilde{v} = \frac{\sqrt{h_R}v_R + \sqrt{h_L}v_L}{\sqrt{h_R} + \sqrt{h_L}} \quad (10)$$
$$\tilde{c} = \sqrt{\frac{g}{2}(h_R + h_L)}$$
$$\tilde{h} = \frac{(h_R + h_L)}{2}$$

To avoid unphysical flow inversion, S_{fx} and S_{fy} in friction term $\mathbf{S}_2$ is discretized in a semi implicit manner:

$$S_{fx}^{*} = 0.5(ghS_{fx})^{k} + 0.5(ghS_{fx})^{k+1}$$
$$S_{fy}^{*} = 0.5(ghS_{fy})^{k} + 0.5(ghS_{fy})^{k+1} \quad (11)$$

Hence, the final numerical equations gained by this scheme is written as:

Published By:
Blue Eyes Intelligence Engineering
& Sciences Publication

$$\mathbf{V}_i^{k+1} = \mathbf{V}_i^k - \frac{\Delta t}{\Delta x}\left(\mathbf{K}_{i+1/2,j} - \mathbf{K}_{i-1/2,j}\right) - \frac{\Delta t}{\Delta y}\left(\mathbf{H}_{i,j+1/2} - \mathbf{H}_{i,j-1/2}\right) + \Delta t(\mathbf{S}^+_{1x(i+1/2,j)} + \mathbf{S}^-_{1x(i-1/2,j)}) + \Delta t(\mathbf{S}^+_{1y(i,j+1/2)} + \mathbf{S}^-_{1y(i,j-1/2)}) + \Delta t \cdot \mathbf{S}_2 \quad (12)$$

C. VALIDATION

1) Flood extents of partial dam break flow

In the years, 2010 and 2011, Aureli and other researchers carried out a new methodology based on image technique to gain experimental data of dam break flow in laboratory of Parma University (Italy). These data are very useful to verify numerical schemes and were also used to this purpose by the same authors, [14].

The configuration of the laboratory tests is shown in Fig. 2. A rapidly varying flow is generated by opening gate instantaneously. Partial dam break flow propagate on horizontal, dry area with obstacle. The initial water depth at upstream of gate is 15cm. An unsubmersible column 30cm×15cm is placed downstream of the gate.

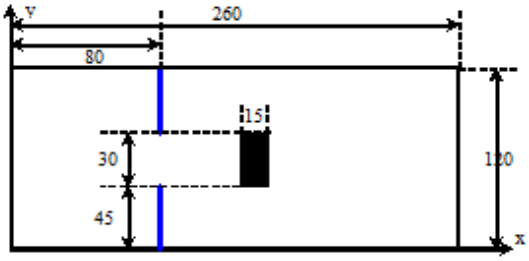

Fig. 1. Sketch of computational domain (dimension in *cm*).

Computational domain is discretized by using a Cartesian grid size 5mm×5mm. Manning coefficient n is set to 0.007. Threshold water depth is imposed by $h_e = 4\times10^{-4}$m and Courant number is Cr = 0.9. Reflective boundary condition is imposed to all sides of the domain.

Water released by gate removal crashes into this obstacle and separated into two parts (see flood maps at t = 0.75*s* and t = 1.45*s*). When t = 2.16s, dam break wave hits two side wall of experimental tank, then it propagates to the downstream end. The back wave resulting by three closed boundaries can be also observed in flood maps at t = 2.86s. This behavior can be seen in both numerical and experimental solutions, (Fig.2). Therefore, the capability of the proposed numerical model in capturing shock wave is very effective and robust.

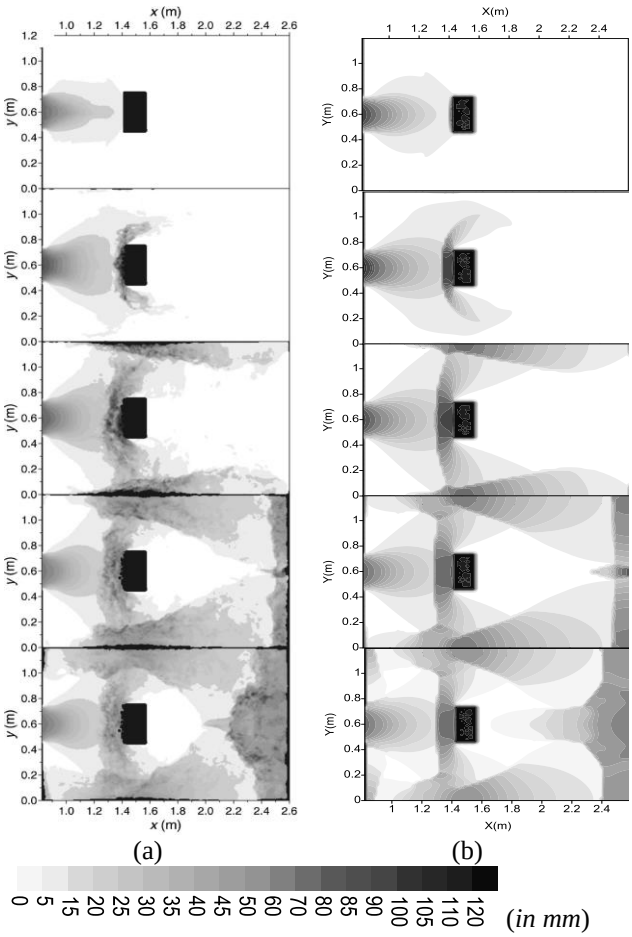

Fig. 2. Flooding maps in downstream at: t = 0.40*s*; t=0.75*s*; t = 1.45*s*; t = 2.16*s*; t = 2.86*s*.
a) Observed data; b) Numerical result.

2) Water depth profile of dam-break flow over horizontal floodable area

In this test, configuration of experiment device is the same as the previous one (Fig. 3). But, water depth profiles at different gauges was collected. The coordinate of six gauge are: G_1 (107, 16) cm; G_2 (107, 60) cm; G_3 (107, 89) cm; G_4 (236, 30) cm; G_5 (236, 60) cm; G_6 (236, 103) cm (see Fig. 3). Initial water depths in the reservoir is 6.3cm and downstream of the gate is dry, [14].

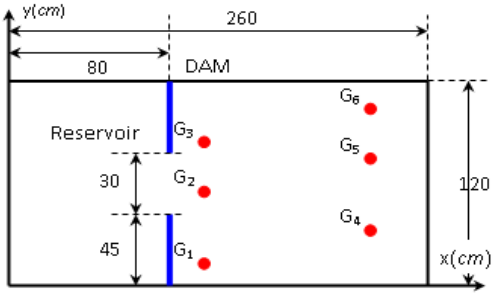

Fig. 3. Configuration of experiment test (dimension in *cm*)

Published By:
Blue Eyes Intelligence Engineering
& Sciences Publication

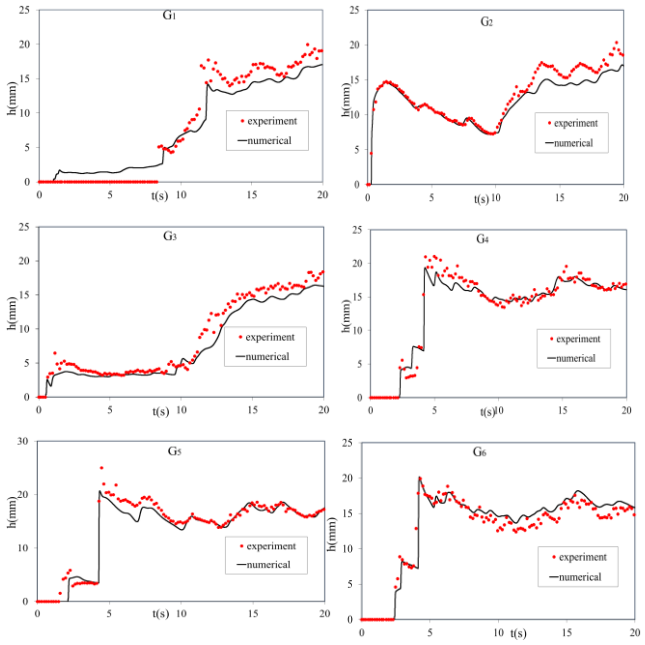

Fig. 4. Water depth profiles at different Gauges.

In the numerical simulation, Manning coefficient n is 0.007 and a grid size Δx=Δy=5mm is used. The computational time is set equal to 20s while the threshold value of water depth is 0.0004m.

Globally, numerical result can capture well the trend of experimental hydrographs in all observed gauges (Fig. 4). The significant overestimation is observed at gauges near dam gate, G_1, G_2 and G_3 during 10s later of computational time. However, a remarkable good matching between computed and measured arrival times to the different gauges is also seen in this figure.

3) Influence of Manning roughness coefficient on flood wave.

Taking to account the impact of friction roughness coefficient on dam-break wave propagation, an interesting test case of 400m×200m horizontal domain bounding by solid vertical walls is reproduced (see Fig. 5), [18]. A dam separates domain into two parts: reservoir and floodplain. Initial water depth is reservoir is 2.0m and floodable area is dry. A partial dam of 20.0m wide will be collapsed suddenly. A 10m-square column is placed in front of dam gate. The quadrilateral mesh size of computational domain is 1.0m×1.0m and Courant number is 0.5.

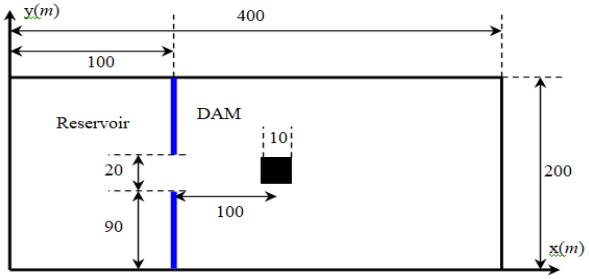

Fig. 5. Plain view of test.

Firstly, Manning coefficient is set equal to 0.011 to simulate the flood extent at different times. According to Fig. 6, at t = 20s, hydraulic jump arrives to the building. As the water spreads onto the floodplain, a depression wave in reservoir travels upstream. 20 seconds later, the flood wave moves around column and then collides with two side walls of computational domain at t = 60s. When t = 150s, dam break wave front propagates to the downstream wall and start to reflect up to upstream. The simulated performance of dam-break wave propagation in both upstream and downstream are quite close with results of Liang's study, while used an explicit TVD-Mac Cormack finite difference method. Therefore, the present numerical model is quite robust and efficient in capturing discontinuous flow over irregular topography.Then, in order to verify the influence of roughness coefficients n, Fig. 7 indicates water hydrograph affected by different Manning values *n* before and after the block. When *n* increases, water depth at gauge before building is reduced while this hydraulic character after building increases gradually. Besides, arrived time of water front reaching these points also reduces. Therefore, this parameter is very important in simulating the propagation of flood wave.

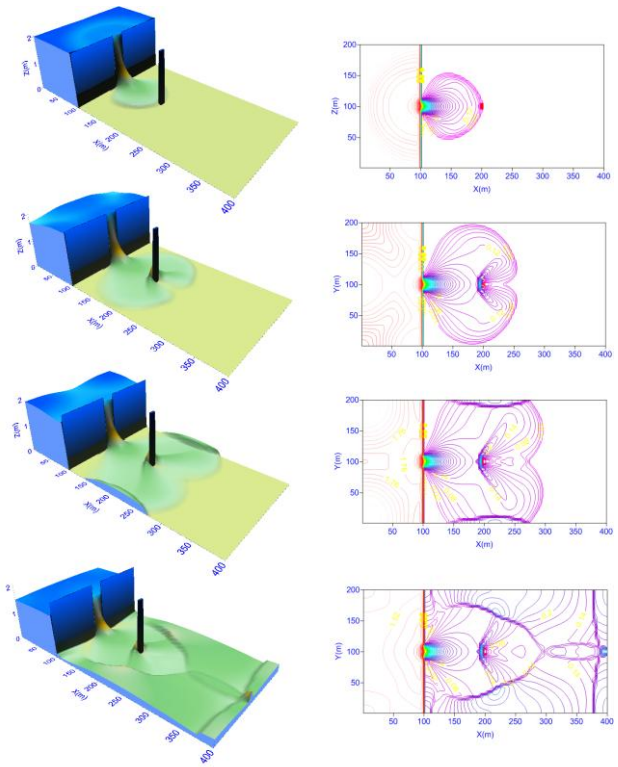

Fig. 6. Flooding maps at: *t* = 20*s; t* = 40*s; t* = 60*s* and *t* = 150*s.*

Published By:
Blue Eyes Intelligence Engineering
& Sciences Publication

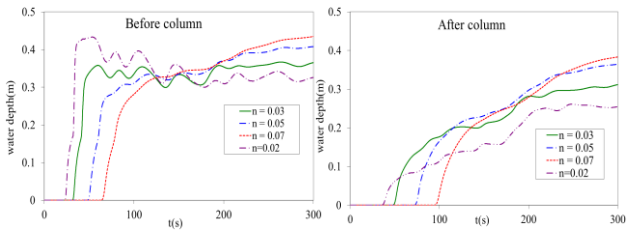

Fig. 7. Water depth hydrographs for different values of Manning coefficient n at two gauges (192, 100)m (before column) and (208, 100) (after column)

III. RESULTS AND DISCUSSIONS

The Nam Chien I hydropower plant is placed on the Chien stream, in Muong La district, Son La province, Vietnam. The project site is located in Da river basin, Chien stream (see Fig. 8). The catchment is located in highland with elevations from 200.0 m to 1900 m a.s.l. The Chien stream is elongated, narrow, 20-35 m wide.

As initial condition, the water surface level corresponding to the normal water elevation (945.0 m a.s.l) is imposed in reservoir, corresponding to a storage volume $V_0 = 154.75.10^6$ m^3. Downstream valley is considered dry. No input discharge is imposed at the upstream end while transmissive condition is used at the downstream boundary. Chien stream is characterized by steep slope bed and high roughness. Accordingly, in the design documentation, the Manning coefficient n is estimated in the range 0.04-0.06 $sm^{-1/3}$. In the numerical simulations, the constant value 0.06 $sm^{-1/3}$ is used. The collected DEM map has regular grid size of 90m×90m. The computational domain fits in a rectangular region of 13000m×14000m. During data collection activity, DEM map and AutoCAD map of both reservoir geometry and head works were acquired.

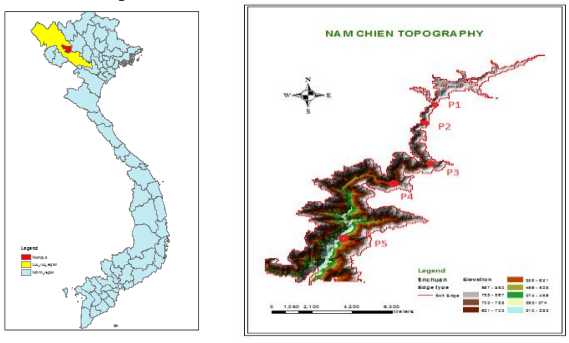

Fig. 8. Namchien's location and topography

The cross section area of arch dam is not so large as well as the downstream valley is quite narrow and steep, (Fig. 9). For this kind of dam, the instantaneous, total collapse is usual dam-break scenario. During the flooding, some bridges and three powerhouses downstream of the dam, namely Nam Chien I, Nam Chien II, Pa Chien are considered to be wiped out.

Different resolutions for simulations are obtained by interpolation. Four uniform grid sizes have been adopted: Δx =Δy = 90m (139×153 cells); Δx = Δy =50m (259×275 cells); Δx = Δy = 40m (320×354 cells); Δx = Δy = 30m (428×460 cells). 5 study points are shown in Fig. 8 where point P_1 is at dam site; point P_5 is location of NamChien powerhouse.

Fig. 9. Nam Chien arch dam (upstream and downstream)

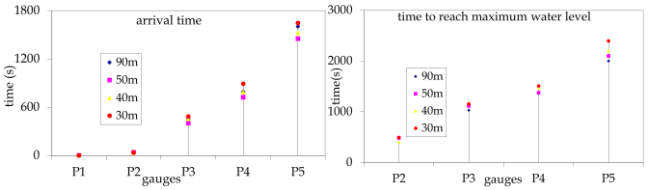

Fig.10. Arrival time and time to reach maximum water level

According to Fig.10, the arrival time of flood wave to 4 study points is predicted by four grid sizes: 30m, 40m, 50m and 90m. The finest grid mesh gives the highest arrival time. Surprisingly, the minimum arrival times are obtained by the coarse mesh with grid size equal to 50m. The arrival times obtained by the different grid sizes at point P_2 near dam site are quite similar. However, at 3 gauges P_3, P_4, P_5, the displacement of these values become greater. Arrival time of flood wave to point P_5 (the powerhouse Nam Chien I) is around 1500s.

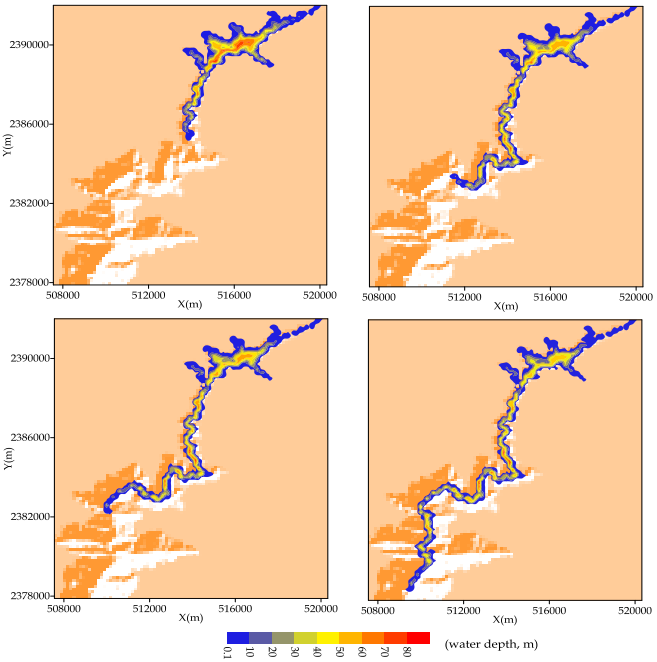

Fig. 11. Flooding maps simulated by Δx = 40 m at: a) t = 300 s; b) t = 1000 s; c) t = 1200 s; d) t = 1700 s.

Besides, the highest values for the time to reach

Published By:
Blue Eyes Intelligence Engineering
& Sciences Publication

maximum water elevation at study gauges are obtained from grid size equal to 30m. The results obtained by both grid sizes 40m and 50m are quite similar. At point P_5, this time is approximately 2200s (see Fig. 10). Hence, when the numerical results obtained by 3 grid resolutions: 30m, 40m, and 50m are quite convergent. Of course, smaller cell size is, longer computation time is used. So, space size 40m is selected to generate inundation maps.

Accordingly, the inundated areas calculated at t = 300 s, t = 1000 s, t = 1200 s and t = 1700 s are shown in Fig. 11. After 1700 s, the dam break wave arrives to the boundary of computational domain (to Nam Chien powerhouse's location).

Therefore, the propose numerical model is able to provide the main information required in dam break analyses aimed at hazard assessment and at the development of early warning plans.

IV. CONCLUSIONS

FVM is selected to solve 2D-SWEs on Cartesian mesh. FDS method is utilized to guarantee correctly balance between fluxes and source terms. Roe scheme is invoked to approximate Riemann problem, while, semi implicit method is implemented to solve friction component in SWE. By three reference tests presented in this paper, the present scheme is demonstrated to have capability of simulating dam-break flow over complex topographies, which can be able to work with real case study. The total dam-break flood flow from NamChien reservoir (Vietnam) is simulated by presented model to obtain several hydraulic characteristics, such as: flooding map, maximum water depth or arrival time at different gauges with different grid sizes. This information is essential to provide an early warning plan for downstream.

REFERENCES

1. F. Aureli and P. Mignosa (2004). Flooding scenarios due to levee breaking in the Po river. Water management. I. 57, 3-12.
2. M. Pilotti, M. Tomirotti, G. Valerio, B. Bacchi (2018). Simplified method for the characterization of the hydrograph following a Sudden partial dam break. J. Hydraulic Engineering. 136(10), 693-704.
3. Vincent Wolfs, Victor Ntegeka, Maria Bermúdez and Patrick Willems (2018). Development of a fast urban flood model for real-time applications. HIC 2018. 13th International Conference on Hydroinformatics,3, 2327-2332.
4. Xilin Xia, Qiuhua Liang, Xiaodong Ming (2018). High-Performance Integrated hydrodynamic Modelling of Storm Induced Floods at a Catchment Scale. HIC 2018. 13th International Conference on Hydroinformatics,3, 2359-2367
5. R.J. LeVeque (1998). Balancing source terms and flux gradients in high resolution Godunov Methods: The quasi steady wave propagation algorithm. J. Computational Physics. 146, 346 – 365
6. E.F. Toro (2001). Shock-capturing methods for free-surface shallow flows, Wiley, Chichester, U.K.
7. A. Valiani; V. Caleffi and A. Zanni (2002). Case study: Malpasset Dam-break Simulation using a two dimensional finite volume method. J. Hydraulic Engineering. 128(5) (ASCE), 460- 472.
8. I.K. Nikolos and A.I. Delis (2009). An unstructured node–centre finite volume scheme for shallow water flows with wet/dry fronts over complex topography. Comput. Methods Appl. Mech. Engrg. 198, 3723 – 3750.
9. J. Hou; Q. Liang; F. Simons; R. Hinkelmann (2013). A stable 2D unstructured shallow flow model for simulations of wetting and drying over rough terrains. Comput. & Fluids. 82, 132–147.
10. J. Hou; Q. Liang; F. Simons; R. Hinkelmann (2013). A 2D well balanced shallow flow model for unstructured grids with novel slope source term treatment. Advances in Water Resources. 52, 107 – 131.
11. Y. Huang; N. Zhang; Y. Pie (2013). Well balanced finite volume scheme for shallow water flooding and drying over arbitrary topography. Engineering Applications of Computational Fluid mechanics. 7(1), 40 – 54.

.